CS180

Vorticity transports in wall turbulent flow under spanwise wall jet forcing and blowing-suction control

Yong Ji[a], Xi Chen[b,*]

[a] College of Science, Harbin Institute of Technology (Shenzhen), Shenzhen 518055, China

[b] Key Laboratory of Fluid Mechanics of Ministry of Education, Beihang University, Beijing, People's Republic of China, 100191

*corresponding author: chenxi97@outlook.com

Abstract

Vorticity transports in wall turbulent flow under blowing-suction (BS) and spanwise opposed wall jet forcing (SOJF) control is studied via direct numerical simulation(DNS). For combining SOJF and BS control, the drag reduction can achieve about 33% - obviously larger than 18% for SOJF and 27% for BS. Following Ji *et al*. [1], the mean spanwise vorticity(Ω_Z), the vorticity fluctuation transports in spanwise direction($-v'\omega_z'$) and normal direction($w'\omega_y'$) are also investigated. A triple decomposition (mean, coherent and random) shows that the role of the random $-v''\omega_z''$ is drag adding, but other terms - random $w''\omega_y''$ and the coherent $-\tilde{v}\tilde{\omega}_z$ and $\tilde{w}\tilde{\omega}_y$ transports – are all drag decreasing.

Introduction

Wall turbulence induces much skin friction drag that contributes approximately 90% of the total drag of underwater vehicles and 50% of commercial aircraft. It is no doubt that the turbulent flow near the wall must be controlled for drag reduction. Yao et al. [2, 3] developed the large-scale drag control concept works by using the near-wall spanwise opposed wall jet forcing (SOJF) and obtained inspiring drag reduction for Reτ up to 550. Chen *et al*.[4] start from energy budget analysis and identified roles of dissipative structures on skin friction. Recently, Ji et al. [1] derived the formula that links the drag coefficient and the motion of the vortical structures, and applied new formula to analyse channel flow under SOJF control. The present work makes DNS about channel flow with SOJF and BS control which yields 33% drag reduction, and analyzes corresponding vorticity transport.

The present work makes direct numerical simulation (DNS) about channel flow with SOJF and BS control which yields 33% drag reduction. Then, the DNS data is analysed by using vortical formula developed in [1]. The results is consistent with previous conclusion that the random spanwise-vorticity transport($-v''\omega_z''$) is only term contributing to drag which should be suppressed for more effective drag reduction

Method

The incompressible Navier-Stokes equation is solved by using open-source software “Incompact3d” [5].

$$\partial u_i / \partial x_i = 0$$

$$\partial_t u_i + \partial_j u_i u_j = \nu \partial_j \partial_j u_i - \partial_i p / \rho + F_i$$

For SOJF, a spanwise forcing is added ,

$$F_z = A_s \sin(\beta z) g(y)$$

The control parameters used are same in ref.[1]. In addition, blowing and suction is applied at bottom and top wall of channel. According to Han & Huang [6], we set $v_{wall} = v_{y+=15}$, where v is wall normal velocity. The no-slip conditions are applied at the walls, and the periodicity in the streamwise and spanwise directions is imposed. In wall normal direction, sixth-order compact schemes are used based on a stretched Cartesian grid. A low-storage third order Runge-Kutta scheme is used to perform time integration. A constant flow rate is set and the bulk velocity Ub is maintained at a constant value by a procedure that adjusts the mean pressure gradient. The simulated Reynolds number Reτ is 180. The Cf at the bottom wall is used to calculate drag reduction R,

$$R = (1 - C_f^{control} / C_f) \times 100\%$$

The decomposition of drag coefficient by vorticity transports is as follow,

$$C_f = \underbrace{\int_0^2 \frac{\varepsilon}{\varepsilon_*} dy'}_{C_\Omega} + \underbrace{\int_0^2 \frac{-\overline{v'\omega_z'}\,\overline{u}}{\varepsilon_*} dy'}_{T_Z} + \underbrace{\int_0^2 \frac{-\overline{w'\omega_y'}\,\overline{u}}{\varepsilon_*} dy'}_{T_Y}$$

$$C_f = \underbrace{\int_0^2 \frac{\varepsilon}{\varepsilon_*} dy'}_{C_\Omega} + \underbrace{\int_0^2 \frac{-\overline{\tilde{v}\tilde{\omega}_z}\,\overline{u}}{\varepsilon_*} dy'}_{T_{Z\text{-}C}} + \underbrace{\int_0^2 \frac{-\overline{v''\omega_z''}\,\overline{u}}{\varepsilon_*} dy'}_{T_{Z\text{-}R}} + \underbrace{\int_0^2 \frac{-\overline{\tilde{w}\tilde{\omega}_y}\,\overline{u}}{\varepsilon_*} dy'}_{T_{Y\text{-}C}} + \underbrace{\int_0^2 \frac{-\overline{w''\omega_y''}\,\overline{u}}{\varepsilon_*} dy'}_{T_{Y\text{-}R}}$$

where the sub-scripts C, R indicate coherent and random motions, respectively. Using Eq. (7), we can separate the drag contributions by other vortical motions and by the large-scale swirls resulted from control.

Table 1. Details of the present direct numerical simulations

Re_τ	Re_b	T	L_x/h, L_z/h	L_x^+, L_z^+	$N_x \times N_y \times N_z$	R
180	2800	800	4π, 2π	2264,1134	192x129x128	27%(BS), 33%(BS+SOJF)

Results

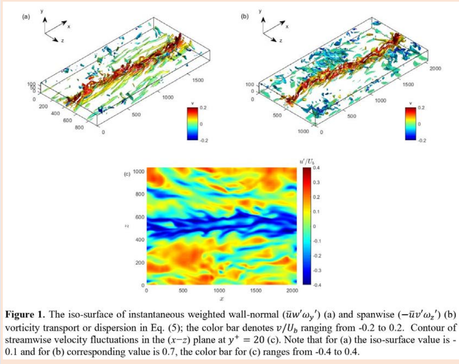

Figure 1. The iso-surface of instantaneous weighted wall-normal ($\tilde{u}w'\omega_y'$) (a) and spanwise ($-\tilde{u}v'\omega_z'$) (b) vorticity transport or dispersion in Eq. (5); the color bar denotes v/U_b ranging from -0.2 to 0.2. Contour of streamwise velocity fluctuations in the (x−z) plane at $y^+ = 20$ (c). Note that for (a) the iso-surface value is -0.1 and for (b) corresponding value is 0.7, the color bar for (c) ranges from -0.4 to 0.4.

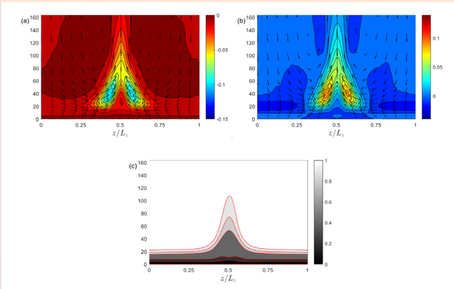

Figure 2. Cross-plane (y−z) view of the mean velocity field ($\tilde{u}$, normalized by U_b) with the contours of $\tilde{u}w'\omega_y'$(a) and−$\tilde{u}v'\omega_z'$ (b) in wall unit, and (c) is the contours of streamwise $< u >_{xt}$ showing the envelop of streaks. Color bar for (a) ranges from 0 to −0.15, for (b) ranges from 0.14 to −0.04, for (c) ranges from 0 to 1.

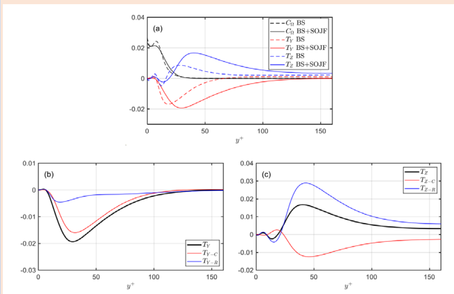

Figure 3. (a) Wall-normal profiles of C_Ω, T_Y and T_Z defined in Eq. (5); Solid lines – BS+SOJF control; dashed lines – only BS control. (b) Wall-normal profiles of T_Y, $T_{Y\text{-}R}$ and $T_{Y\text{-}C}$ defined in Eq. (7). (c) wall-normal profiles of T_Z, $T_{Z\text{-}R}$ and $T_{Z\text{-}C}$ defined in Eq. (7)

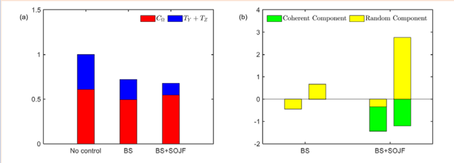

Figure 4. (a) Bar chats of C_Ω, T_Z and T_Y for uncontrolled and controlled cases. (b) Triple decomposed $T_{Y\text{-}R}$ and $T_{Y\text{-}C}$ (left bar), $T_{Z\text{-}R}$ and $T_{Z\text{-}C}$ (right bar).

- Figure 4(a) show that, before control, C_Ω is 61% and Ty+Tz is 39%; after BS control C_Ω is 50% and Ty+Tz is 23%; after BS+SOJF control, C_Ω is 53% and Ty+Tz is 14%.
- Figure 4(b) shows the coherent and random decomposition of Ty (left bar) and Tz (right bar) for BS and BS+SOJF control, respectively. The random component Tz-R is only term contributing to drag under BS+SOJF.

Conclusion

[Following the idea of composite active drag control [7], we investigate the vorticity transport in turbulent channels under BS and BS+SOJF active control. The decomposition of friction coefficient based on vorticity transport is examined. We find that BS+SOJF control perform a better drag reduction (33%) compared to individual BC control (27%) or individual SOJF control (18%). Under the BS+SOJF control, the contribution of different vorticity transport terms to total drag coefficient is similar with our previous result [1] that T_{Z-R} is only term in charge of drag friction, other terms play a role in drag reduction. This analysis suggests that the suppression of random spanwise-vorticity transport is still the target for effective drag reduction under composite control including SOJF.

References

[1] Y. Ji et al. Physics of Fluids. 33. 095112(2021).
[2] J. Yao et al., Physical Review Fluids 2 (2017).
[3] J. Yao, X. Chen, and F. Hussain, Journal of Fluid Mechanics 852, 678 (2018).
[4] X. Chen et al. Phys. Rev. Fluids 6, 013902 (2021).
[5] S. Laizet and E. Lamballais, JCP, 228, 5989(2009)
[6] B.Z. Han and W. X. Huang, Phys. Fluids 32, 095108 (2020)
[7] J. Yao, X. Chen, and F. Hussain, Phys. Rev. Fluids 6, 054605(2021)